Biomaterials 79 (2016) 1–14

Contents lists available at ScienceDirect

Biomaterials

journal homepage: www.elsevier.com/locate/biomaterials

Tailored and biodegradable poly(2-oxazoline) microbeads as 3D matrices for stem cell culture in regenerative therapies

Steffen Lück [a, b, c], René Schubel [a], Jannick Rüb [a, c], Dominik Hahn [c, d], Evelien Mathieu [b], Heike Zimmermann [d], Dieter Scharnweber [d], Carsten Werner [c, d], Sophie Pautot [b, **], Rainer Jordan [a, b, c, *]

[a] Professur für Makromolekulare Chemie, Department Chemie, Technische Universität Dresden, Mommsenstr. 4, 01069, Dresden, Germany
[b] Center for Regenerative Therapies Dresden (CRTD), Fetcherstr. 105, 01307, Dresden, Germany
[c] Dresden Initiative for Bioactive Interfaces & Materials, Technische Universität Dresden, Mommsenstr. 4, 01069, Dresden, Germany
[d] Max-Bergmann Center of Biomaterials Dresden, Budapester Str. 27, 01069, Dresden, Germany

ARTICLE INFO

Article history:
Received 24 July 2015
Received in revised form
9 November 2015
Accepted 29 November 2015
Available online 2 December 2015

Keywords:
Poly(2-oxazoline)
Microbeads
Microfluidics
Biodegradable
Stem cells

ABSTRACT

We present the synthesis of hydrogel microbeads based on telechelic poly(2-oxazoline) (POx) crosslinkers and the methacrylate monomers (HEMA, METAC, SPMA) by inverse emulsion polymerization. While in batch experiments only irregular and ill-defined beads were obtained, the preparation in a microfluidic (MF) device resulted in highly defined hydrogel microbeads. Variation of the MF parameters allowed to control the microbead diameter from 50 to 500 μm. Microbead elasticity could be tuned from 2 to 20 kPa by the POx:monomer composition, the POx chain length, net charge of the hydrogel introduced via the monomer as well as by the organic content of the aqueous phase. The proliferations of human mesenchymal stem cells (hMSCs) on the microbeads were studied. While neutral, hydrophilic POx-PHEMA beads were bioinert, excessive colonization of hMSCs on charged POx-PMETAC and POx-PSPMA was observed. The number of proliferated cells scaled roughly linear with the METAC or SPMA comonomer content. Additional collagen I coating further improved the stem cell proliferation. Finally, a first POx-based system for the preparation of biodegradable hydrogel microcarriers is described and evaluated for stem cell culturing.

1. Introduction

Polymer microbeads are spherical hydrogel particles on the micrometer or sub-micrometer scale and are considered as discrete, crosslinked gel particles made of polymers [1,2]. In the last decades, a steadily rising interest emerged since microbeads are applicable in a large field of interest, comprehensively reviewed by Snowden and co-workers [3], due to their enormous diversity in size, structure and physicochemical properties. Whether as drug delivery devices [4] or as three-dimensional scaffolds for cell culturing [5,6], microbeads are playing an important part in biomedical research and development. Therefore many possible materials, microbeads can be made off, like glass, poly(*N*-isopropylacrylamide) (PNIPAAm), poly(styrene) (PS), dextran, gelatin, poly(ethylene gycol) (PEG) or poly(lactic-*co*-glycolic acid) (PLGA) have been extensively studied for use as microcarriers, microspheres or delivery vehicles [6–13] but most materials lack in certain criteria of biocompatibility, adjustability or versatility. Hence, poly(2-oxazoline)s (POx) are gaining more and more interest due to their favorable properties. POx are prepared by living cationic ring-opening polymerization (LCROP) of 2-substituted-2-oxazolines resulting in defined polymers of low molar mass distribution [14]. Depending of the 2-substitution on one hand the water-solubility can be adjusted from highly hydrophilic (2-methyl-) or slightly amphiphilic being comparable to polyethylene glycol (PEG) [15,16], to highly hydrophobic (e.g. 2-nonyl-) [17,18], on the other hand reactive side-chains can be easily introduced by using functional monomers [19–23]. Furthermore different polymer architectures like star-polymers [24,25], or

* Corresponding author. Professur für Makromolekulare Chemie, Department Chemie, Technische Universität Dresden, Mommsenstr. 4, 01069, Dresden, Germany.
** Corresponding author.
E-mail addresses: sophie.pautot@crt-dresden.de (S. Pautot), Rainer.Jordan@tu-dresden.de (R. Jordan).

http://dx.doi.org/10.1016/j.biomaterials.2015.11.045
0142-9612/

molecular brushes [26–29] are accessible. The hydrophilic poly(2-methyl-2-oxazoline) PMeOx and poly(2-ethyl-2-oxazoline) PEtOx were found to be non-toxic [16,30], showed very low to no complement activation [31], a fast renal excretion [32] and POx-conjugates exhibit the so called "stealth effect" very similar to PEGylated compounds [16,33]. These properties renders POx as a very promising polymer for the design of biomaterials [34–36]. One implementation is the use as POx-based hydrogels and numerous different designs emerged in the last decades, extensively investigated by Wiesbrock and co-workers [37] and recently summarized by Schubert et al. [38] to create e.g. thermoresponsive [34], pH- and reductive-responsive [39] or degradable [40] networks. However, only few efforts were made to explore and investigate POx-based hydrogel particles in a biomedical context. David et al. [41] reported on the fabrication of particles made of PNiPAAm, PMeOx/PEtOx and 2-hydroxyethyl methacrylate (HEMA) by a precipitation technique receiving particles in the range of 30–200 nm and size distributions of 1.05–1.15 and their use as drug delivery vehicle. Zschoche et al. [42] synthesized poly(NIPAAm-graft-(2-alkyl-2-oxazoline)) nanogels by crosslinking self-assembled micelles. Recently, Taton and Lecommandoux et al. [43] obtained nanogels by crosslinking of partially hydrolyzed PEtOx. Spherical oxazoline-based fluorescent particles with diameters ranging from 650 to 750 nm and narrow size distributions were successfully prepared by Jerca et al. [44]. However, all particles reported to date are in the sub-micrometer size range with the potential use as systemic drug-delivery systems. In the view of the chemical and physical versatility of POx-based materials, an intriguing field of application is their use as substantially larger but defined microbeads or microcarriers for cell cultivation and especially in regenerative therapies.

In the present study we describe for the first time the fabrication of POx-based hydrogel microbeads by means of emulsion polymerization in batch as well as in a microfluidic system. While batch synthesis resulted in microbeads of irregular shapes with inclusions and broad size distributions, synthesis with a microfluidic setup [45] resulted in highly regular spherical particles of very narrow size distributions and allowed precise control of the particle diameters from over a broad range from 50 to 500 μm [46,47]. In order to tailor crucial microgel properties, we aimed for a highly modular and tunable system that allows defined control over microgel size and composition to modulate relevant chemical and physical properties. Besides the microbead size, chemical composition and charge, we also tuned the microbead stiffness by the crosslinking density of the gels [48] to address the impact of mechanosensing of adhered (stem) cells [49–52]. Our modular system successfully allowed to modulate the adhesion of human mesenchymal stem cell (hMSC) on the microbeads as a function of their chemical composition, charge and surface chemistry [51,53]. Finally, we introduced a cleavable disulfide bond into the telechelic POx crosslinkers for triggered microbead disintegration to enable cell harvesting under mild physiological conditions with glutathione.

2. Experimental section

2.1. Materials and methods

All chemicals were purchased from Sigma–Aldrich (Weinheim, Germany) or Acros (Renningen, Germany) and used as received unless otherwise stated. Acetonitrile (ACN), triethylamine (TEA) and 2-methyl-2-oxazoline (MeOx) were refluxed over CaH_2 and distilled under nitrogen prior to use. The initiator *trans*-1,4-dibromo but-2-ene (DBB) was recrystallized from dry acetone and dried in vacuum before use. 2-Hydroxyethyl methacylate (HEMA), methacrylic acid (MAA) and propargyl p-toluenesulfonate (P-OTs) have been purified by distillation under nitrogen.

Human bone marrow stromal cells (hMSCs) were isolated from the iliac crest of healthy males (20 and 37 years old) and kindly provided by the Medical Clinic I, Dresden University Hospital Carl Gustav Carus, Germany.

Gel permeation chromatography (GPC) was performed with a PL-GPC 120 using dimethyl acetamide (DMAc) as eluent that contained 5 g/L LiBr and 1% Milli-Q water with a flow rate of 1 mL/min at 70 °C. We used a precolumn (GRAM, 8 mm × 50 mm, 10μ) and two GRAM 1000 columns (8 mm × 300 mm 10μ)) by PSS (Mainz, Germany) for sample separation. The injection volume was 100 μL and a refractive index (RI) detector was used for detection. The system was calibrated against PMMA standards (PSS, Mainz, Germany) in the range of 600 to 67,000 g/mol. MALDI-ToF-MS was performed on a Biflex IV from Bruker Daltonics. Sample preparation was executed as following; a solution of 1 mg/ml analyte in methanol containing 0.1 vol% trifluoroacetic acid was mixed with a saturated solution of sinapinic acid in methanol in a ratio of 1:5 and 1 μL was placed on the target. The system was calibrated against the peptide calibration standard II (Bruker) at sample conditions. ^1H NMR spectroscopy was performed on a Bruker DRX 500 P at 500 MHz and 298 K, using $CDCl_3$ and DMSO-d6 as solvents. The spectra were calibrated to the TMS signal. Gas chromatography (GC) was performed on a Varian 430-GC equipped with a CombiPal robot and an Agilent Factor Four VF-5ms column (30 m 0.25 mm, 0.25 μm), at isobaric conditions (10.00 PSI), nitrogen as carrier gas and a FID for detection. Colloidal probe spectroscopy (CPS) was performed with an Ntegra Aura (NT-MDT, Moscow, Russia) atomic force microscope (AFM) on the swollen microbeads in Milli-Q water using a modified liquid cell. The cantilever (k = 0.14 nN/nm in air) was equipped with a home-made colloidal probe tip made from a solid glass bead with a diameter of 10 μm which was attached to the cantilever with the help of a nanomanipulator. For each data point 5 to 10 microbeads per batch were investigated by measuring thrice at 5 different points on each individual bead with 15 s approach and 15 s retreat time. Thus, per batch 75 to 150 individual measurements were performed. Measurements with inconsistent force–distance curves resulting from movement of the microbead during the probing or unsuitable spherical interaction were disregarded.

2.2. Kinetic studies for the telechelic POx synthesis

In a glove-box a mixture of the initiator (DBB or P-OTs), ACN as solvent, chlorobenzene as internal standard and MeOx (2.9 M) was filled into a 10 mL GC vial and sealed with a crimper. After collection of the first sample at t = 0 s the mixtures were shaken at 70 °C using an agitator device. Samples of 1 μL were alternately taken after 11 min and injected by an autosampler.

2.3. Synthesis

Disulfid-diazide was synthesized from a solution of 11 g (49 mmol) of cystamine hydrochloride in 100 mL Milli-Q water adjusted to pH 9 with 1.5 N NaOH and cooled to 0 °C. Chloroacetyl chloride (2.5 eq) was added drop-wise while the pH value was maintained between 7 and 9 with NaOH. After 3 days stirring at room temperature the colorless precipitate was filtered, wash with Milli-Q water and dried over P_2O_5 under vacuum (2.5×10^{-2} mbar). The obtained colorless powder was dissolved in 100 mL DMF and 2.5 eq sodium azide was added step-wise. The mixture was stirred overnight at 60 °C and subsequently diluted in 125 mL DCM and 200 mL Milli-Q. The organic phase was separated, washed thrice with 80 mL Milli-Q water and the organic solvents were removed

under vacuum. The yellowish residue was precipitated in ice-cold ether, filtered and dried under high vacuum. This procedure gave a colorless powder with a yield of 33%. ^{1}H NMR (500 MHz, DMSO-d_6, 298K): δ 8.31 (t, N**H**, J_{23} = 5.38), 3.86 (q, CH_2–C**H$_2$**–NH, J_{12} = 6.48, J_{23} = 12.87), 3.83 (s, CO–C**H$_2$**), 2.80 (t, S–C**H$_2$**, J_{12} = 6.78).

Poly(2-methyl-2-oxazoline)-dimethacrylate (PMeOx$_n$) was synthesized under dry and inert conditions from a mixture of 1 eq DBB as the initiator and n (10 or 30) eq MeOx at 70 °C in ACN ([MeOx] = 2.9 M). The reaction was terminated with a 2.5-fold excess of MAA and TEA after calculated reaction time, stirred overnight at 60 °C and neutralized with K_2CO_3. The polymer product was precipitated twice and lyophilized to give a colorless powder with a yield of 83%. ^{1}H NMR (500 MHz, $CDCl_3$, 298K): δ 6.08 (=C**H$_2$**), 5.6 (=C**H$_2$**), 5.6 (m, =CH–C**H$_2$**–N), 4.28 (m, C**H$_2$**–COO), 3.94 (m, =C**H**-), 3.49 (m, N–C**H$_2$**–C**H$_2$**), 2.16 (m, CO–C**H$_3$**), 1.91 (m, CH_2=C–C**H$_3$**).

Alkyne-endfunctionalized poly(2-methyl-2-oxazoline)-methacrylate (P-PMeOx$_n$) was synthesized as described above with P-OTs as the initiator and adjusting the reaction time to the different rate constants. After work-up a colorless powder with a yield of 90% was obtained. ^{1}H NMR (500 MHz, $CDCl_3$, 298K): δ 6.08 (=C**H$_2$**), 5.6 (=C**H$_2$**), 4.28 (m, C**H$_2$**–COO), 4.11 (m, C–CH2–N), 3.49 (m, N–C**H$_2$**–C**H$_2$**), 2.29 (s, H–C≡C), 2.16 (m, CO–C**H$_3$**), 1.91 (m, CH_2=C–C**H$_3$**)

Poly(2-methyl-2-oxazoline)-disulfide-dimethacrylate (PMeOx$_n$-DS) was obtained by copper-catalyzed azide-alkyne cycloaddition (CuAAC) of **P-PMeOx$_n$** and the **disulfide-diazide**. Therefore, 2 eq of **P-PMeOx$_n$** were coupled with 1 eq of the **disulfide-diazide** in the presence of 10 eq ascorbic acid and 0.6 eq of $CuSO_4$ at ambient temperature in Milli-Q water. After subsequent dialysis (MWCO 1000 kDa) a white powder could be obtained with yield 95%. ^{1}H NMR (500 MHz, DMSO-d_6, 298K): δ 8.53 (m, N**H**), 8.09–7.88 (m, N–C**H**=C), 6.01 (s, =C**H$_2$**), 5.69 (m, =C**H$_2$**), 5.06 (m, CO–C**H$_2$**–N) 4.55 (m, =C–C**H$_2$**–N), 4.19 (m, C**H$_2$**–COO), 3.42 (m, S–CH_2–C**H$_2$**–NH, N–C**H$_2$**–C**H$_2$**), 2.75 (m, S–C**H$_2$**–CH_2), 2.0 (m, CO–C**H$_3$**), 1.89 (m, CH_2–C=C**H$_3$**)

2.4. Hydrogel microbead preparation

2.4.1. Emulsion polymerization in batch

In a darkened environment, a mixture of the telechelic POx crosslinker (**PMeOx$_n$** or **PMeOx$_n$-DS**), monomer (HEMA, METAC) and 143 mg ammonium persulfate were dissolved in degassed Milli-Q water (freeze–pump–thaw cycled) to form the aqueous phase. The solution was filtered (0.24 μm) and purged with nitrogen prior to use. Different ratios of the POx crosslinker to monomer were used to obtain different network structures. The oil phase was prepared from 250 mL dodecane and 1 g surfactant (SPAN80) was filled into a stirring reactor (Rettberg, Göttingen, Germany) equipped with a heating shell to maintain a constant temperature of 25 °C and purged with nitrogen under moderate stirring. After 30 min the stirring was stopped and the oil phase was equilibrated for 15 min to eliminate the nitrogen gas bubbles. Afterwards a constant stirring rate of 300 rpm was adjusted and the aqueous phase was added constantly using a syringe. Droplets were formed spontaneously and after 30 min 100 μL TEMED was added. After 4 h the gelation was completed, the mixture centrifuged, the oil phase removed and the microbeads dialyzed (5 kDa MWCO) against Milli-Q water for 4 days. The prepared microbeads were stored in Milli-Q water for further use.

2.4.2. Emulsion polymerization in a microfluidic system

A microfluidic (MF) device was prepared according to the protocol of Whitesides et al. [45]. In short, MF structures were designed with an open source CAD program (Inkscape) and printed as a negative onto a transparency with a high-resolution printer. We used various designs and dimensions of the MF device, including T-junction, flow focusing and varied the orifice dimensions from 100 to 175 μm as well as the injection angle (60° or 90°) at a fixed channel width of 625 μm. For most of the hydrogel microbeads presented here, an optimized design with T-type junctions and 625 μm channel width at 60° channel angle was used. This transparency was used as a mask for photolithography to produce a master from a copper based circuit board covered with a photoresist. After development, poly(dimethylsiloxane) (PDMS, RTV615, MG Chemicals, New Mills, U.K.) was casted onto the master and cured according to the literature [45] to build a polymeric replica containing the channel structures. Tubing inlets to connect the MF structure to the pumps were stamped out and the MF device completed with a smooth PDMS plate. The obtained PDMS device was connected to syringe pumps (type HLL LA-03 from Landgraf Laborsysteme, Langenhagen, Germany). As in the batch procedure, the aqueous phase was formed by dissolving the polymeric crosslinker and monomer (HEMA, METAC, SPMA) with a saturated solution of the photo initiator (IRGACURE®, BASF Ludwigshafen, Germany) in degassed Milli-Q water. The aqueous phase was purged with nitrogen as well as the oil phase made from paraffin oil and 4 g/L surfactant (SPAN80). Oil and aqueous phases were loaded into each syringe pump of the MF device. Different flow rates for the water phase from 0.75 to 3.5 μL/min and the oil phase from 300 to 1250 μL/min were used to control particle size and to maintain a constant droplet formation (see main text). The droplets were collected in stirring tank and crosslinked with UV light using a 200 W Hg lamp (type LSN265 from LOT-QuantumDesign, Darmstadt, Germany). After 2 h irradiation the mixture was drained, centrifuged, the oil phase removed and the microbeads dialyzed (5 kDa MWCO) for 4 days against Milli-Q water. Finally, microbeads were sieved through a 600 μm mesh-strainer to remove bead clusters. Additionally, when microbeads were prone to be used for cell culture the beads were sieved through a 120 μm mesh to remove endocytotic available particles. The purified microbeads were finally stored in Milli-Q water for further use.

2.5. Microbead preparation for cell adhesion studies and collagen coating

2.5.1. Native microbeads

Under sterile conditions (clean bench with laminar flow), 500 mg swollen microbeads were placed into 50 mL FALCON tube and sterilized by replacing the water with 10 mL 70% ethanol for 10 min while slightly shaking. Then, ethanol was replaced by 30 mL sterile phosphate buffered saline (PBS) and shaken for another 10 min. Washing was repeated twice, and PBS replaced by 10 mL medium (Dulbecco's modified eagle medium (DMEM), 3.7 g/L $NaHCO_3$, 1 g/L D-glucose) without further fetal bovine serum (FBS) added to improve cell adhesion according to the results of Yuan et al. [9]. The tubes were left unsealed but covered for at least 15 min in a cell incubator (37 °C, 8% CO_2) for equilibration.

Collagen coated microbeads were obtained as described above but by replacing the PBS buffer with 2 mL of a collagen solution (3 g/L in 10 mM HAc). Afterwards, the microbeads were shaken for 1 day with a NeoLab® Intelli-Mixer to avoid microbead settlement. Finally, all mircobeads were transferred under sterile conditions into new tubes. After thrice washing with 10 mL 10 mM HAc, the samples were incubated in FBS-free DMEM and stored under sterile conditions for further use. The resulting collagen content was determined by hydroxyproline assay according to Reddy et al. [54].

2.6. Cell culture with human mesenchymal stem cells (hMSC)

After microbead preparation and collagen coating, each sample was inoculated with 0.5 million hMSCs (P6) for each 500 mg microbead batch and placed ajar in the incubator. During the first 4 h post-inoculation, an intermittent shaking was applied by manual shaking for some seconds followed by 30 min without shaking following a procedure described by Yuan et al. [9]. Afterwards, 20 mL tempered full medium (DMEM + 0.2 mM L-glutamine + 1% PIS + 10% FBS) was added and samples were cultured for 7 days without further shaking but careful medium exchange after the 4th day. Cell attachment was investigated by bright field and fluorescence microscopy (Axio Observer. Z1m, equipped with an AxioCam MRm all from Carl Zeiss Microscopy GmbH, Jena, Germany) and quantified via lactate dehydrogenase assay (LDH). All cell culture reagents were purchased from Biochrom GmbH, Berlin, Germany except FBS (from Lonza Group, Köln, Germany).

2.7. Lactate dehydrogenase assay (LDH)

After incubation, medium was aspirated and microbeads washed with warm PBS through a 70 μm sieve to separate non adhered cells from the microbeads. Microbeads were quantitatively transferred into a 70 μm mesh-strainer in a 6-well-plate, covered with 5 mL tempered trypsin and incubated at 37 °C for 15 min. Immediately after incubation time, 5 mL full-DMEM (37 °C) was added, sieves slightly shacked and transferred on a 50 mL FALCON tube. The remaining liquid in the plate was used to wash the beads and to transfer detached cells in the tube. Another 5 mL full-DMEM (37 °C) was used to wash the 6-well-plate and to quantitatively transfer all cells into the tube. The mesh-strainer with the microbeads were dried, weighed and washed again to remove the microbeads, dried and weighed again to yield the exact mass of microbeads used in the experiment. The tubes with the cells were centrifuged for 5 min at 0.4 G, the medium aspirated, 2 mL warm PBS added, again centrifuged, the PBS aspirated and stored at −80 °C for at least 1 day before the LDH assay (TaKaRa LDH Cytotoxicity Detection Kit, MoBiTec, Göttingen, Germany).

The LDH assay translates into cell numbers by external calibration using 500, 1,000, 2,000, 5,000, 10,000 and 20,000 cells.

2.8. Cell staining

Cultured cells on microbeads were washed with warm PBS, fixed with 3.7% formaldehyde (PBS) for 25 min at 4 °C and washed again with cold PBS. Cells were permeabilized in 0.1% Triton-X and slightly shaken for 3 min, washed thrice with PBS and incubated with 1% (v/v) BSA in PBS for 30 min to avoid unspecific binding. Afterwards, the samples were incubated with a mixture of 6 μM phalloidin (Alexa 488) and 1 μg/mL DAPI in 1% (v/v) BSA/PBS and slightly shaken in the dark for 30–60 min. Finally, microbeads were washed thrice with 1% (v/v) BSA/PBS. DAPI staining of SPMA containing microbeads was not possible because of high DAPI uptake of the negatively charged beads.

2.9. Degradation of $PMeOx_{30}$-DS microbeads by glutathione or sodium borohydride

2.9.1. Microscopy studies at physiological GSH concentration

Under nitrogen, a suspension of 1 g degradable microbeads (30-1-M-DS) in 50 mL degassed Milli-Q water containing GSH was slightly stirred at 37 °C. Degradation by 2.8 μM GSH was monitored by optical microscopy on sample fractions taken after indicated time intervals. The change of the microbead elasticity upon degradation by 10 mM GSH was examined *in situ* by CPS on individual microbeads.

2.9.2. CPS studies at higher GSH concentration

Under argon, a degassed dispersion of 30-1-M-DS in 10 mM GSH was placed in a closed AFM liquid cell from NT-MDT. One microbead was selected and the Young's modulus was determined at indicated time intervals by CPS using a tip and set-up as described above. CPS was performed on several beads without noticeable deviations of the results. Data on one representative continuous experiment is shown in the main text.

2.9.3. Degradation for SEC measurements

Under argon, 1 g 30-1-M-DS microbeads were subjected to reductive decomposition using either 10 mM or 2.8 μM glutathione (GSH) or 0.5 M sodium borohydride (all in 50 mL degassed Milli-Q water) under nitrogen at 37 °C for 5 days. The crude final solution was analyzed by SEC using a BioSep-SEC-S 2000 column (Phenomenex, USA) with PBS (pH 7.4) as eluent at a flow rate of 0.5 mL/min and UV–vis detection at a wavelength of 210 nm. The system was calibrated with a set of PMeOx homopolymer standards in the range from 0.95 to 16.5 kg/mol to calculate the respective molar mass from the elution time. Standards were synthesized by LROP using methyltriflate as the initiator, MeOx monomer and piperidine as the termination agent as described elsewhere [22,30]. PMeOx standards were characterized by endgroup analysis based on ^{1}H NMR spectroscopy data and MALDI-ToF-MS. Standards used were:

Polymer standard	M_{MALDI} (g/mol)	Dispersity ($Đ = M_w/M_n$)
$PMeOx_9$	949	1.19
$PMeOx_{19}$	1800	1.12
$PMeOx_{27}$	2482	1.15
$PMeOx_{50}$	4536	1.15
$PMeOx_{93}$	8119	1.14
$PMeOx_{200}$	16500	1.65

3. Results and discussion

3.1. Synthesis of POx crosslinkers

There are several possibilities to synthesize a POx-based hydrogels and to combine it with a second polymer for further property tuning [38]. In our design we wanted to take advantage of the precise molecular engineering of POx and use the polymer as a telechelic polymer crosslinker to modulate the gel elasticity as well as to introduce a biodegradable group within the POx chain. The preparation of the hydrogel should be reliable and applicable for emulsion type polymerization to allow formation of beads. Hence, a telechelic POx equipped with methacrylic end groups had to be synthesized and copolymerized with methacrylates by free radical (photo)polymerization. For the microbead preparation, we adopted the synthesis of bulk POx hydrogels as reported by Du Prez et al. [55,56], using α,ω-functionalized POx. The telechelic POx was synthesized from *trans*-1,4-dibromo but-2-ene (DBB) as the initiator [57] for the living cationic ring-opening polymerization (LCROP) of 2-methyl-2-oxazoline (MeOx) and methacrylic acid as the terminator (Fig. 1a) [56,58–59]. The crosslinking density of the resulting gels was varied by either the length of the POx crosslinker, adjusted by the MeOx to DBB ratio, and/or later by a different ratio of the POx crosslinker to the methacrylic comonomers in the free

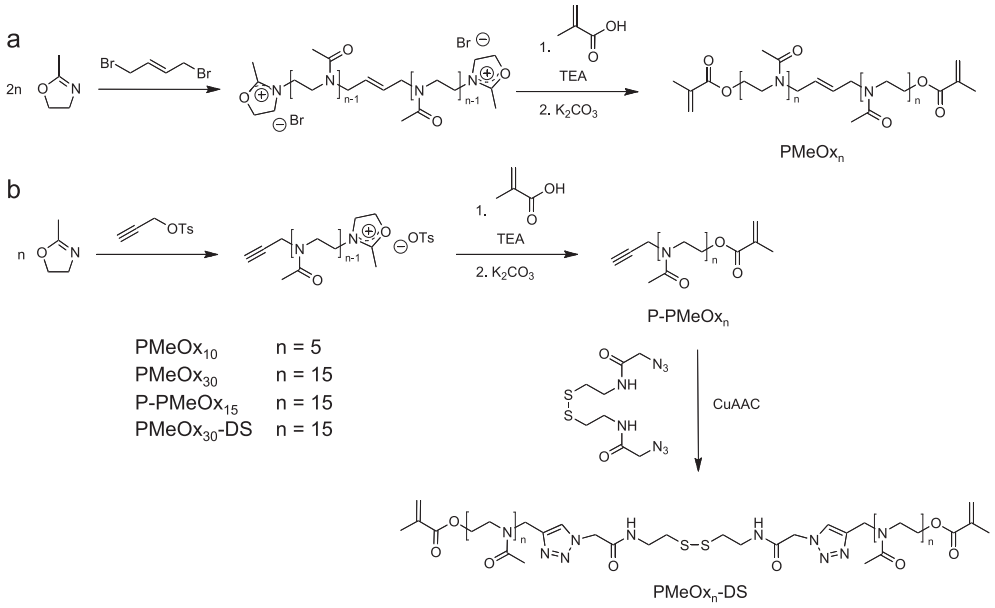

Fig. 1. Synthesis of telechelic methacrylate functionalized poly(2-methyl-2-oxazoline) ($PMeOx_n$, total length of 2n = 10, 30) crosslinkers using a) *trans*-1,4-dibromo but-2-ene as a bisfunctional initiator. Incorporation of a biodegradable disulfide linker was realized by b) click-reaction of an α-alkyne-ω-methacrylate POx ($P\text{-}PMeOx_n$) and a subsequent click-reaction with a disulfide-diazide compound to yield $PMeOx_n$-DS with a total length of 2n = 30.

radical polymerization.

To incorporate a biodegradable linker into the hydrogel microbeads, first, a clickable POx ($P\text{-}PMeOx_n$) was synthesized equipped with a proximal alkyne and a distal methacrylate group with propargyl p-toluenesulfonate (P-OTs) as the initiator [25], again, MeOx as the monomer for LCROP and methacrylic acid as the terminator. The complete linker with a central disulfide group (PMeOx-DS) was assembled by quantitative copper catalyzed alkyne azide cycloaddition (CuAAC) with a disulfide-diazide compound (Fig. 1b). As POx crosslinkers, $PMeOx_n$ and $PMeOx_n$-DS were used in the consecutive emulsion polymerization. Both linkers were set to the same length having 10 or 30 MeOx units in total.

The LCROP of MeOx with both initiators was investigated by kinetic studies as previously reported [24] to elucidate the stoichiometric living polymerization characteristics of the initiator systems. The resulting first-order kinetic plots (Fig. 2) showed a good linear behavior up to high monomer conversions as expected for a highly living polymerization system. For DBB, an apparent polymerization rate of k_p^{app} of 2.1 mmol/L and an effective rate constant per initiating group of 1.06 mmol/L was found; P-OTs gave a k_p^{app} of 1.43 mmol/L at 70 °C and a monomer concentration of 2.9 M. This relates to a reaction time of approx. 95 min for the conversion of 10 monomer units ($PMeOx_{10}$) and 4 h for 30 monomer units ($PMeOx_{30}$) for DBB initiation and 80 min for $P\text{-}PMeOx_{15}$, respectively. As expected, the rate constants of a tosylate initiator are higher than for a halide such as bromide because of the lower nucleophilic character of the gegenion during the LCROP. With the use of the kinetic behavior, telechelic POx could be synthesized in high yields, low dispersities, Đ, and maximum fidelity with respect to the end functionalization, F. As apparent from Table 1, in all cases the determined POx chain length could be successfully adjusted by the initial monomer to initiator ratio ($[M]_0/[I]_0$).

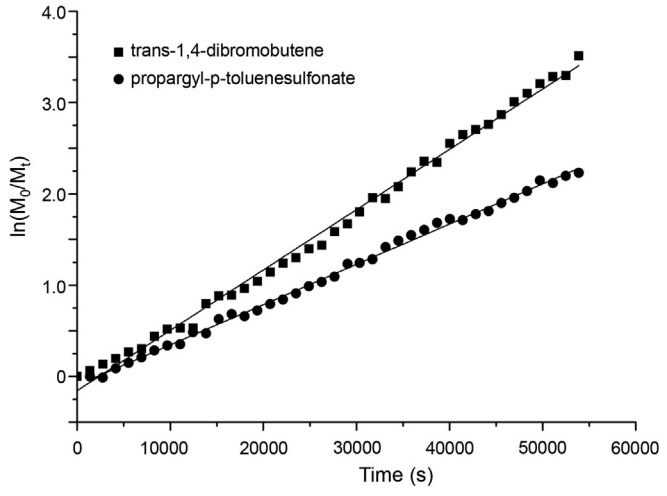

Fig. 2. First order kinetic plots for the polymerization of 2-methyl-2-oxazoline (MeOx) with *trans*-1,4-dibromo but-2-ene or propargyl p-toluenesulfonate as the initiator ([MeOx] = 2.9 M, T = 70 °C in ACN).

The resulting molar masses are in a good agreement with the calculated masses except the masses of the alkyne-bearing POx received from the GPC investigation to show slightly higher molar masses. This shifted elution time is most probably due to an unspecific interaction of the polymer via the end group with the stationary phase which results in a shift to an apparent higher molar mass. From the MALDI-ToF-MS spectrum of $P\text{-}PMeOx_{15}$, a good agreement between targeted and obtained average molar mass was found. Detailed analysis of all polymers by GPC, ^{1}H NMR spectroscopy and MALDI-ToF-MS confirmed the structures as outlined in Fig. 1. The ^{1}H NMR spectra of $P\text{-}PMeOx_{15}$ and after the CuAAc of $PMeOx_{30}$-DS are displayed in Fig. 3a and b along with the GPC traces before and after the click reaction (Fig. 3c). In the ^{1}H NMR spectra, all signals could be assigned according to the literature especially indicating the high endgroup functionalization [25] and comparison of the GPC traces indicates a quantitative click-reaction.

3.2. POx-based microbeads

For the fabrication of hydrogel microbeads several methods are

Table 1
Analytical data of telechelic POx crosslinkers.

Polymer	$[M]_0/[I]_0$	n[a]	M^{calc} [g/mol]	M_n[b] [g/mol]	M_p[c] [g/mol]	F[a] [%]	Đ[b]
$PMeOx_{10}$	10	10	1075	1050	1247	95	1.19
$PMeOx_{30}$	30	30	2777	2860	3074	93	1.27
P-$PMeOx_{15}$	15	15	1400	1870	1474	97	1.17
$PMeOx_{30}$-DS	30	33	3120	4870	3489	96	1.12

[a] Determined by endgroup analysis from ^{1}H NMR spectroscopy data.
[b] Determined by GPC, $Đ = M_w/M_n$.
[c] Determined by MALDI-ToF-MS.

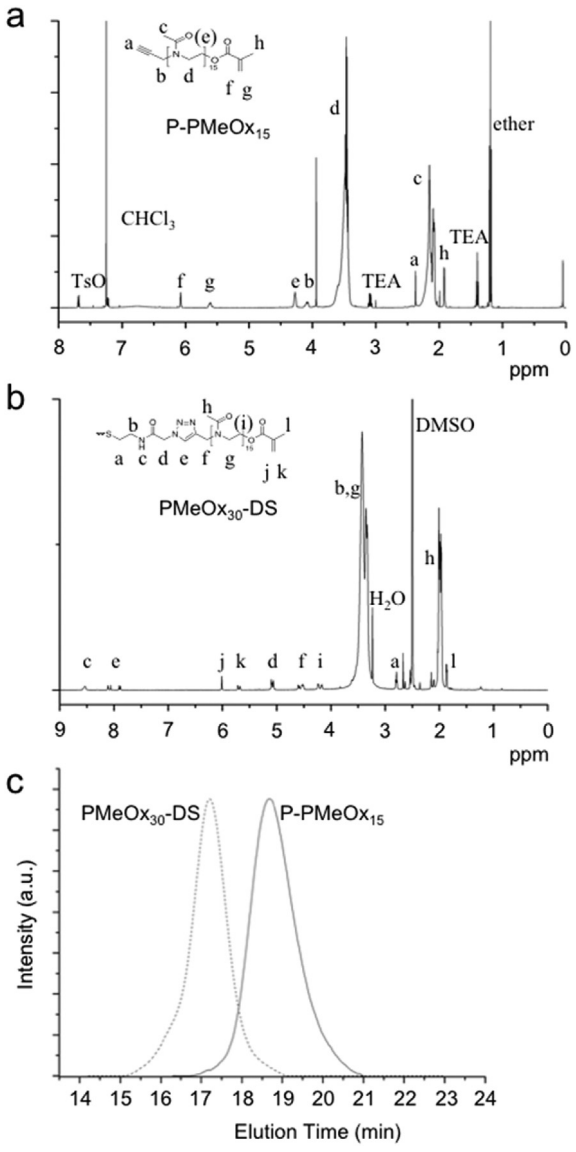

Fig. 3. ^{1}H NMR spectra of a) P-$PMeOx_{15}$ and b) $PMeOx_{30}$-DS as well as c) GPC traces of P-$PMeOx_{15}$ and $PMeOx_{30}$-DS conforming quantitative conversion of P-$PMeOx_{15}$ to $PMeOx_{30}$-DS by CuAAC.

available such as dispersion, precipitation and inverse emulsification techniques, spray drying, or coacervation leading to various particle sizes and distributions [60]. As we aimed for a modular and scalable method we first investigated the conventional method by w/o emulsion polymerization in batch to yield microbeads from the water phase containing the POx crosslinker, comonomers and a redox initiator in oil (dodecane) and an emulsifier (SPAN80) by mechanical agitation and free radical polymerization to form the hydrogel particles in the water droplets. As monomers we selected the hydrophilic 2-hydroxyethyl methacrylate (HEMA), the positively charged [2-(methacryloyloxy)ethyl]trimethylammonium chloride (METAC) and the negatively charged sulfopropyl methacrylate (SPMA) to elucidate the effect of the comonomers charge upon the microbead elasticity as well as the cell adhesion. Variation of the crosslinker length ($PMeOx_{10}$, $PMeOx_{30}$ and $PMeOx_{30}$-DS) and comonomers to crosslinker ratio should vary the resulting average arc-length of the hydrogel and thus, the gel elasticity. Moreover, the concentration of polymerizable compounds in the water phase (organic content %) should result in thin (soft) or denser (stiffer) hydrogels. Indeed, the batch emulsion polymerization with e.g. $PMeOx_{10,30}$ and HEMA as the comonomer readily resulted in stable hydrogel microbeads of various sizes which could also be tuned by the stirring speed. However, inspection of the beads by optical microscopy (Fig. 4a–e) revealed the formation of irregular particles with inclusions and protrusions (Fig. 4c), very broad dispersities (Fig. 4d) and inhomogeneous cores (i.e. double emulsions). Moreover, it was planned to additionally coat the microbeads by proteins in a consecutive step to modulate later cell adhesion by optimizing the particle surface properties. For batch synthesized microbeads, fluorescence-labled BSA was used in an assay to investigate protein-particle interaction and coating possibilities. Microbeads from batch showed inhomogeneous staining (Fig. 4e) and are thus not useful for consecutive coating procedures. We accounted the problems of emulsion polymerization in batch to an inefficient and inhomogeneous formation of the aqueous droplets by stirring, adhesion and/or association of droplets or partially polymerized gels during the crosslinking reaction. Variation of reaction conditions including change of the emulsifier or emulsifier content, oil phase (n-heptane, paraffin, dodecane) did not significantly improve the microbead morphology to a degree that would allow a later systematic investigation.

An intriguing alternative to produce hydrogel microbeads of defined morphology, narrow size distribution, tunable sizes and even various shapes is their formation by microfluidics in which an aqueous phase is constantly injected into a flow of oil to form droplets of defined sizes in the range of tens to some hundreds of micrometers [1,12,46,61]. Such devices are relatively easy to prepare by rapid prototyping using PDMS [45]. We therefore fabricated and tested various microfluidic (MF) devices made from PDMS connected to two syringe pumps, one injecting the aqueous phase as described above into a continuous flow of paraffin oil to create defined aqueous droplets in series. The droplets were collected in a reservoir and the hydrogel matrix was obtained by free radical photopolymerization of POx crosslinkers and comonomers with the aid of a photoinitiator (IRGACURE®) and an UV lamp illuminating the reservoir. For most designs we readily obtained stable and very uniform hydrogel particles but most reliably with a simple T-junction geometry with 625 μm channel width and various flow rates to control the particle size. An injection angle of 60° was found to be ideal for the droplet formation and to avoid that the oil

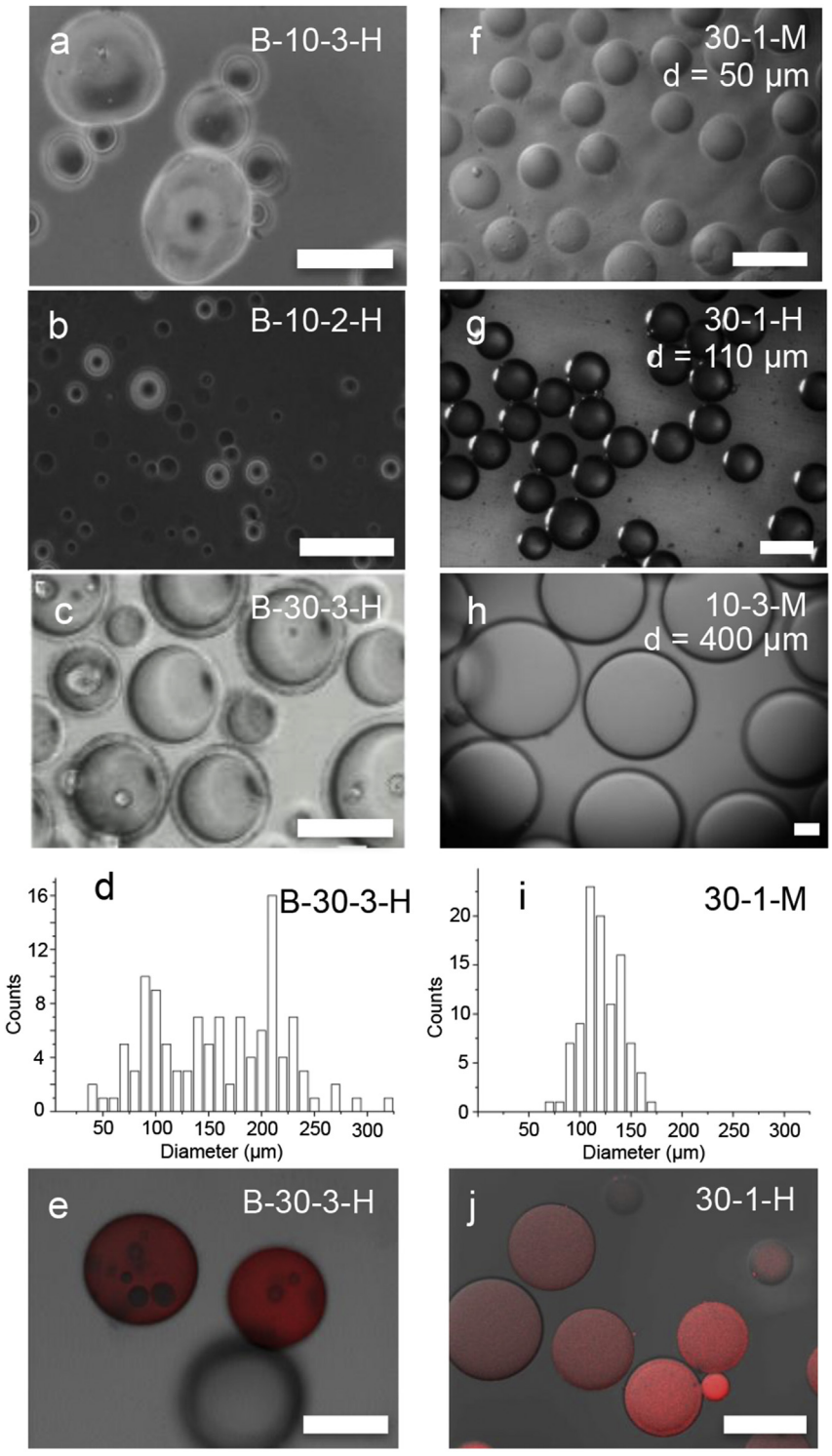

Fig. 4. Comparison of POx-based hydrogel microbeads prepared by emulsion polymerization in batch (a–e) and in a microfluidic (MF) device (f–j). Bright-field optical micrographs of batch synthesized particles (a–c) revealed the formation of irregular and inhomogeneous particles of a broad size distribution. Exemplarily, the particle size distribution of B-30-3-H is shown (d) with a PDI of 1.143 and particles with an average diameter of 153 ± 60 µm but ranging from 30 to 320 µm. Microbeads prepared by MF were spherical with a narrow size distribution (PDI = 1.026) (i). Fluorescence microscopy of rhodamine-BSA coating of the microbeads showed inhomogeneous coating for microbeads prepared in batch (e) whereas MF microbeads allowed homogeneous staining (j). Please note that the BSA coating could be removed by washing because of the low particle protein interaction. For MF, the particle diameters could be adjusted in a wide range by the variation of the flow rates and flow rate ratio of the oil:water phase (see Table 2). Scale bar in all micrographs is 100 µm.

phase is pressed into the water guiding channel. Selected examples of hydrogel microbeads prepared by MF are depicted in Fig. 4e–h along with their typical size distribution Fig. 4i as determined by image analysis of optical micrographs. Moreover, incubation with rhodamine-BSA resulted in homogeneous staining of the particles (Fig. 4j), indicating a uniform coating, which renders the

microbeads suitable for consecutive coating procedures. Besides the significantly improved microbead uniformity, it is noteworthy that microbead fabrication by microfluidics is readily scalable as it can be performed in a continuous process. In our case, the microbead output is in the range of 1.5–2 g/h.

The general reaction scheme for the preparation of hydrogel microbeads by emulsion polymerization in batch and in a MF device is outlined in Fig. 5 along with the abbreviations for the respective particles used for the measurements of the elasticity of the hydrogel microbeads as well as later cell cultivation experiments.

Table 2 summarizes selected examples of microbeads prepared by MF under variation of the used POx crosslinker ($PMeOx_{10,30}$: 10- or 30-; with an additional disulfide: -DS) monomer (-H: HEMA; -M: METAC) and their respective ratio in wt% (POx crosslinker:monomer -1-: 70/30, -2-: 50/50, -3- 30/70) at different flow rates and flow rate ratios.

For entries 1 to 6 the crosslinker, monomer and composition was fixed (30-1-M) and the flow rates for the oil and water phase was varied in a wide range in order to tune the average diameter of the microbeads. As apparent, the sizes of the microbeads could successfully be tuned from 60 to 480 μm and in all cases spherical, homogeneous microbeads of narrow size distributions were readily obtained. Smaller as well as much larger microbeads with a diameter of 20 μm or beyond 500 μm were obtained with different MF designs and conditions, however, as the first aim of this work was the preparation of microcarriers for the cultivation of human mesenchymal stem cells, these approaches will be subject of future studies. The particle diameter was a direct function of the water phase flow rate, however, in order to realize relatively small or big particles also the flow rate of the oil phase had to be modified to ensure a constant droplet injection at the T-junction. Thus, the flow rate ratio is additionally listed to show the flow rate–size correlation. This correlation is not valid for other compositions (entries 7 to 24) as the viscosity of the aqueous phases as well as the contact angle upon contact with the oil phase changes significantly for different crosslinker:monomer compositions and crosslinkers used.

Entries 7 to 24 lists the MF conditions for materials prepared from different POx crosslinker chain lengths and crosslinker:monomer ratios to vary the hydrogel arc-length which should yield microbeads of different stiffness. Moreover, two different monomers (HEMA and METAC) were used to study the influence of charges in the hydrogel upon the microbead elasticity and finally, for a given composition the organic content in the aqueous phase was varied. Only for one case (30-3-H, entry 11), we could not obtain stable hydrogel microbeads because the high HEMA content resulted in an incomplete crosslinking reaction within the aqueous droplets.

The last column lists the Young's modulus of the microbeads as determined by colloidal probe spectroscopy (CPS). CPS was performed according to Butt et al. [62,63], using the Hertz equation to calculate the Young's modulus from the force–distance curves. For batch synthesized materials, CPS did not give reproducible results as measurements on individual beads from the same batch gave very different Young's moduli and a representative value for a single batch could not be determined thus, only CPS results from microbeads prepared by MF are given. In Fig. 6a the Young's moduli are compared for the different POx crosslinker length, used monomer and crosslinker to monomer ratio measured for different individual beads from the same batch. For both PMeOx crosslinkers, the hydrogel becomes systematically softer for increased contents of the hydrophilic HEMA. This is expectable because of the increase of the average gel arc-length formed by PHEMA by the UV polymerization. However, increase of crosslinker length results not in a softer but significantly stiffer material (10.5 kPa for 10-1-H *vs.* 22 kPa for 30-1-H) but differences are smaller for higher HEMA contents (6.2 kPa for 10-2-H vs. 13 kPa for 30-2-H). This might indicate a better incorporation of the longer $PMeOx_{30}$ crosslinker into the PHEMA hydrogel network as for the longer POx crosslinker the comparison of the elasticity with PMETAC materials also shows an overall higher Young's modulus. However, as PMeOx-co-PHEMA microbeads displayed no significant protein adsorption or cell adhesion in studies described below, this aspect was not further investigated. For METAC containing material, the trends are as

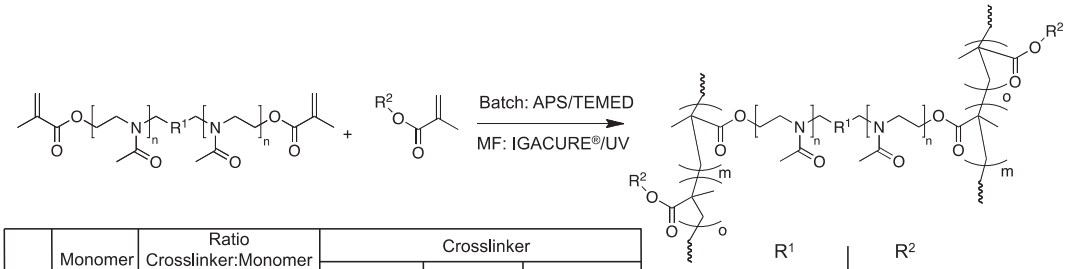

	Monomer	Ratio Crosslinker:Monomer [wt%]	Crosslinker		
			$PMeOx_{10}$	$PMeOx_{30}$	$PMeOx_{30}$-DS
Batch	HEMA	70 : 30	B-10-1-H	B-30-1-H	-
		50 : 50	B-10-2-H	B-30-2-H	-
		30 : 70	B-10-3-H	B-30-3-H	-
Microfluidics (MF)	HEMA	70 : 30	10-1-H	30-1-H	30-1-H-DS
		50 : 50	10-2-H	30-2-H	-
	METAC	70 : 30	10-1-M	30-1-M	30-1-M-DS
		50 : 50	10-2-M	30-2-M	30-2-M-DS
		30 : 70	10-3-M	30-3-M	30-3-M-DS
	SPMA	70 : 30	10-1-S	30-1-S	30-1-S-DS
		50 : 50	10-2-S	30-2-S	30-2-S-DS
		30 : 70	10-3-S	30-3-S	30-3-S-DS

Fig. 5. Preparation of hydrogel microbeads by emulsion polymerization in batch with ammonium persulphate/tetramethylethylenediamine (APS/TEMED) and by microfluidics (MF) using IGACURE® as the photoinitiator and UV irradiation. With different POx crosslinker lengths (10, 30) and variation of the crosslinker:monomer ratio, the gel density was controlled. As comonomers either HEMA, METAC or SPMA were used. Furthermore, POx crosslinkers with a disulfide core ($PMeOx_{30}$-DS) were incorporated to yield biodegradable microbeads.

Table 2
Characterization of microbeads prepared by emulsion polymerization in a microfluidic device (MF device type: T-junction, 625 μm channel width at 60° angle and flow rates for the oil and water phase as indicated). For all entries the organic content, OC (POx and monomer), was 30 wt% unless otherwise stated.

#	Microbeads (OC, wt%)	Composition POx/Monomer (wt%)	Flow rate (μL/min) oil:water	Flow rate ratio	Diameter (μm)[a]	DispersityPDI[b]	Young's modulus (kPa)[c]
1	30-1-M	70/30	1250:1.5	833	59 ± 13	1.0427	n.d.
2	30-1-M	70/30	950:1.5	633	141 ± 13	1.0077	n.d.
3	30-1-M	70/30	650:1.5	433	219 ± 15	1.0051	n.d.
4	30-1-M	70/30	1250:3.5	357	370 ± 16	1.0002	n.d.
5	30-1-M	70/30	350:2.9	120	426 ± 12	1.0001	n.d.
6	30-1-M	70/30	350:3.5	100	476 ± 14	1.0001	n.d.
7	10-1-H	70/30	400:1	400	154 ± 15	1.0085	10.5 ± 1.7
8	10-2-H	50/50	50:0.5	25	122 ± 37	1.0166	6.2 ± 0.8
9	30-1-H	70/30	200:1.5	133	184 ± 13	1.0064	21.8 ± 6.5
10	30-2-H	50/50	250:0.75	333	184 ± 15	1.0372	13.2 ± 2.4
11	30-3-H	30/70	various	various	no beads	–	–
12	30-1-H-DS	70/30	750:0.75	1000	219 ± 17	1.0064	4.6 ± 1.7
13	10-1-M	70/30	400:1	400	185 ± 11	1.0029	14.4 ± 6.9
14	10-2-M	50/50	350:1	350	191 ± 13	1.0041	15.1 ± 2.9
15	10-3-M	30/70	400:0.8	500	145 ± 11	1.0058	16.5 ± 5
16	30-1-M	70/30	400:0.75	533	222 ± 16	1.0073	5.6 ± 1
17	30-2-M	50/50	300:0.75	400	260 ± 16	1.0041	8.7 ± 1.6
18	30-2-M (20%)	50/50	400:0.75	533	233 ± 20	1.007	6.7 ± 2.1
19	30-2-M (10%)	50/50	400:0.8	500	281 ± 23	1.006	2.5 ± 0.8
20	30-2-M (7.5%)	50/50	400:0.75	533	316 ± 22	1.007	2.1 ± 0.7
21	30-3-M	30/70	400:1	400	267 ± 15	1.0054	11.9 ± 3.8
22	30-1-M-DS	70/30	300:1	300	161 ± 10	1.0039	2.3 ± 1.2
23	30-2-M-DS	50/50	300:1	300	160 ± 6	1.0018	4 ± 1.9
24	30-3-M-DS	30/70	300:1	300	187 ± 10	1.0028	5.9 ± 2.3

[a] Determined by image analysis of optical micrographs, ± = standard deviation.
[b] PDI = d_n/d_d.
[c] Determined by colloidal probe microscopy, ± = standard deviation.

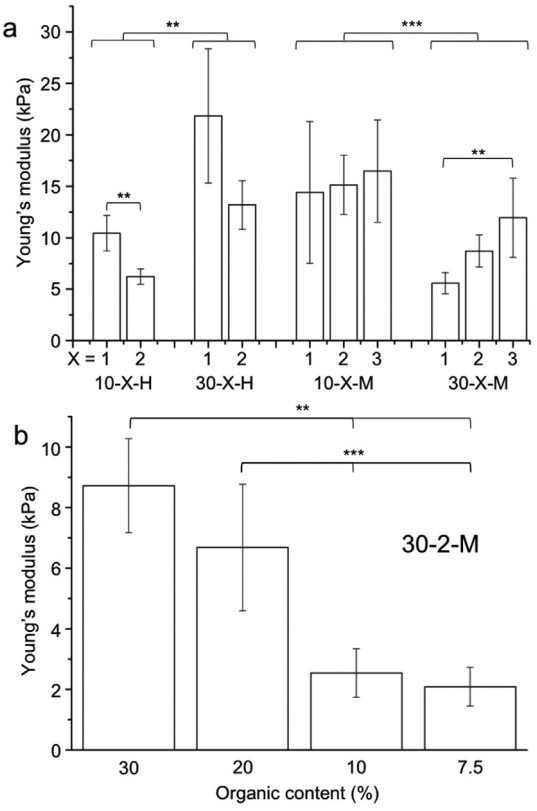

Fig. 6. Elasticity of the microbeads as probed by colloidal probe spectroscopy. a) Young's modulus as a function of POx crosslinker length, monomer type and POx crosslinker:monomer composition for organic content of 30%. b) Modulation of the elasticity by variation of the organic content from 30 to 7.5 wt% for 30-2-M type hydrogel microbeads. Values are presented as mean (n = 3–16) ± S.D., $^{**}p < 0.05$, $^{***}p < 0.01$ using Student's *t*-test.

expected. A longer POx crosslinker gives softer materials, while more METAC stiffens the material as incorporation of more METAC introduces more positive charges into the gel and the coulomb repulsion of the PMETAC polyelectrolyte results in a systematic stiffening of the hydrogel microbeads. In this series the elasticity of microbeads could be systematically tuned from 5 to 22 kPa. Materials described till now (entries 1–17 and 21–24) were prepared with an organic content (POx crosslinker and monomer) of 30 wt% in the aqueous phase. Additionally, for entries 17 to 19 in Table 2, the organic content was systematically changed from 30 to 7.5 wt% for 30-2-M type materials. Fig. 6b shows the significant reduction of the Young's modulus as a function of the organic content. With this additional parameter, the Young's modulus could be systematically reduced from 9 kPa (30 wt%) to a very soft hydrogel of 1–2 kPa for 7.5 wt% organic content without change of the chemical composition of the material.

In conclusion, by the variation of the composition, monomer, used POx crosslinker and organic content, microbeads with Young's moduli from 1 to 2 kPa up to 22 kPa are accessible. In early studies, Discher et al. [50,64], pointed out that the elasticity of hydrogel substrates plays a significant role in the cell differentiation of adhered stem cells. Although later studies gave a more detailed picture [52] this specific aspect will be subject of own future studies using the here described microbeads because the POx chemistry readily allows incorporation of additional adhesion motifs as well as growth factors by chemical ligation as recently demonstrated by Dargaville et al. [65]. With the microbeads described in this study, fully synthetic and well controlled 3D matrices of very different elasticity mimicking soft, brain like tissue, muscle up to collagenous material are now accessible in a facile and reproducible manner.

3.3. Cultivation of human mesenchymal stem cells (hMSCs)

The suitability of the hydrogel microbeads synthesized by MF for the cultivation of cells was investigated in order to evaluate their potential in regenerative therapies. We studied the

proliferation of human mesenchymal stem cells (hMSCs) onto the POx-based microcarriers as bone marrow derived hMSCs are an ideal cell source for numerous regenerative therapies and tissue engineering [66,67].

For the cell studies, we synthesized microcarriers under variation of the POx crosslinker, monomer (HEMA, METAC and SPMA), crosslinker:monomer ratios but of comparable particle diameter around 410 ± 10 μm to exclude effects of the microcarrier geometry such as the particle curvature, area per particle and different interparticle volumes. This was relatively easy by adjusting the flow rates of the oil and water phase in the microfluidic device.

For each microbead type, 500 mg portions of microbeads were incubated for 7 days with hMSCs, not adhered cells were removed. The hMSC colonization of the microbeads was carefully quantified by LDH assay. Fig. 7 gives the average number of hMSCs on the respective microbeads.

For POx-HEMA beads (30-1-H and 30-2-H), no cell adhesion and later proliferation was observed because their highly hydrophilic nature rendered them bioinert. In contrast, microbeads containing positively charged PMETAC showed excessive hMSC colonization and very high numbers of proliferated stem cells. Interestingly, the cell number reached a maximum for POx-METAC beads with a crosslinker:monomer ratio of 50:50 at 341 × 10^4 and 363 × 10^4 cells/g, respectively, independent of the crosslinker length and microbead stiffness (15.1–8.7 kPa). We observed no significant difference within (X = 1,2,3) or between (10 or 30) for the POx-METAC samples. For the 10-2-S type microbeads a significantly higher cell number was found as compared to the 30-X-S series and the 10-3-S sample. Comparison of microcarriers prepared with METAC and SPMA comonomers, however, showed significant differences ($p < 0.01$) in cell counts which can be explained by the net charge of the beads being positive (METAC) or negative (SPMA). We found that hMSCs proliferation is up to 7 times better on positively charged microbeads such as 30-2-M (340 × 10^4 cells/g) as compared to 30-2-S (47 × 10^4 cells/g). This is in good agreement to previous studies that revealed significantly higher hMSC proliferation on positively charged PAH-terminated polyelectrolyte multilayers comparing to negatively charged PSS-terminated ones due to thicker and denser fibronectin layers on the surface and thus a better hMSC adhesion [68,69].

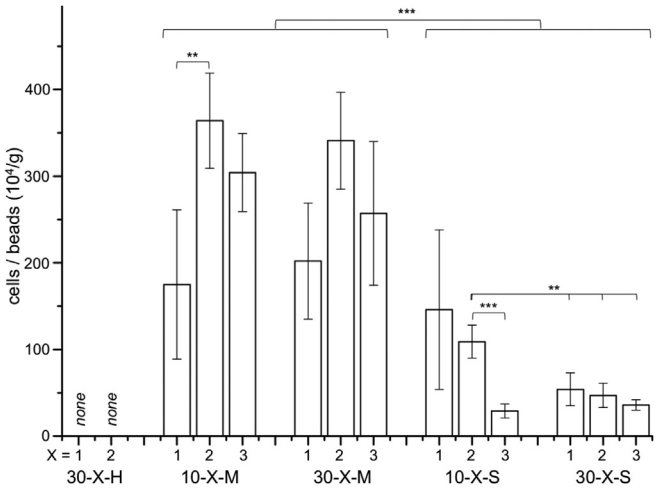

Fig. 7. Colonization of POx-based MF-microbeads composed from short (10: $PMeOx_{10}$) or long (30: $PMeOx_{30}$) POx crosslinkers and hydrophilic neutral (H: HEMA), positive (M: METAC) and negative (S: SPMA) monomers of different crosslinker:monomer ratios (1: 70:30; 2: 50:50; 3: 30:70) by hMSCs as quantified by an LDH assay after 7 days incubation time. Cell numbers are presented as mean (n = 3) ± S.D., $^{**}p < 0.05$, $^{***}p < 0.01$ using Student's *t*-test.

The hMSCs on all microcarrier types prepared with HEMA, METAC and SPMA comonomers with the same $PMeOx_{30}$ crosslinker was investigated by fluorescence microscopy using DAPI as nucleus marker, and phalloidin (Alexa 488) as F-actin marker.

Fluorescence microscopy of fixed and stained cells (Fig. 8c) revealed very good cell adhesion and effective cell spreading around the charged hydrogel microcarriers. We also observed that hMSCs started to populate the interparticle spaces and attached onto two or more microcarriers simultaneously. Analysis of several fluorescent micrographs revealed excessive colonization of up to 50 hMSC cells on a single 30-1-M microcarrier of an average diameter of 490 μm. Fig. 8c also shows that hMSCs do not populate POx-HEMA microbead surfaces. Additionally, the influence of an adhesion promoting coating of the microbeads was investigated and native as well as collagen type I coated cells were compared as collagen type I presents optimal ligands for the cell adhesion of hMSCs [66].

As apparent from Fig. 8 not only hMSC colonization was suppressed for the PMeOx-PHEMA (30-1-H) type material, also attempts to coat the bioinert material with collagen I was not successful and only minor amounts of collagen I could be determined by the hydroxyproline assay. Consequently, the proliferation of hMSCs on 30-1-H beads did not significantly improved. The pure hydrophilic PMeOx-PHEMA microbeads are thus unsuitable for cell culturing [70,71]. However, this non-biofouling behavior of PMeOx-PHEMA microbeads might prove to be highly interesting for the use of the material in another biotechnological context. On positively charged PMeOx-PMETAC (30-3-M) microbeads, 200 μg/g collagen I could be deposited and negatively charged PMeOx-SPMA (30-3-S) microbeads were coated efficiently with 400 μg/g as collagen I exhibit a net positive charge [66]. The proliferation of hMSCs on the native positive PMeOx-PMETAC as well as on the negatively charged PMeOx-PSPMA is high and in terms of cells/mass beads (around 60 × 10^4 cells/g microcarriers) and cell spreading very similar. The additional collagen I coating further improves the hMSC proliferation but most significantly for 30-3-S as their high PSPMA content results in a high negative net charge which allows efficient collagen I deposition and thus stronger adhesion promotion for hMSCs. For the collagen coated $PMeOx_{30}$-PSPMA material, the LDH assay gave a very high cell population of 140 × 10^4 cells per gram microbeads after an incubation time of only 7 days.

It is noteworthy that the cell culture studies performed with the POx-based microbeads were rather facile because the beads could be effectively dispersed during the cell incubation phase by slight agitation but readily settled as individual particles when left unstirred. Moreover, the uniform beads assemble as relatively stable colloidal crystals, which allows a facile exchange of the aqueous phases for culture media exchange or during the washing steps without disturbing the microbead/cell assembly. All microbeads were found to be thermally stable and could be autoclaved prior to the cell studies. In summary, the POx-based microbeads were found to be a robust and easy to handle 3D matrix system for the cultivation of stem cells.

3.4. Biodegradable hydrogel microbeads for regenerative therapy

Major obstacles for effective regenerative therapies is the efficient *ex vivo* expansion of stem cells on 2D or 3D scaffolds [9] as well as their transfer into a living organism under preservation of their cell character. Both aspects might be addressable by the use of POx-based hydrogel microcarriers as 3D cultivation scaffolds. However, even after a successful transplantation of injectable microcarriers populated by stem cells, the synthetic scaffolds then remain in the organism and might cause local infections or cause complement activation if they are not sufficiently bioinert.

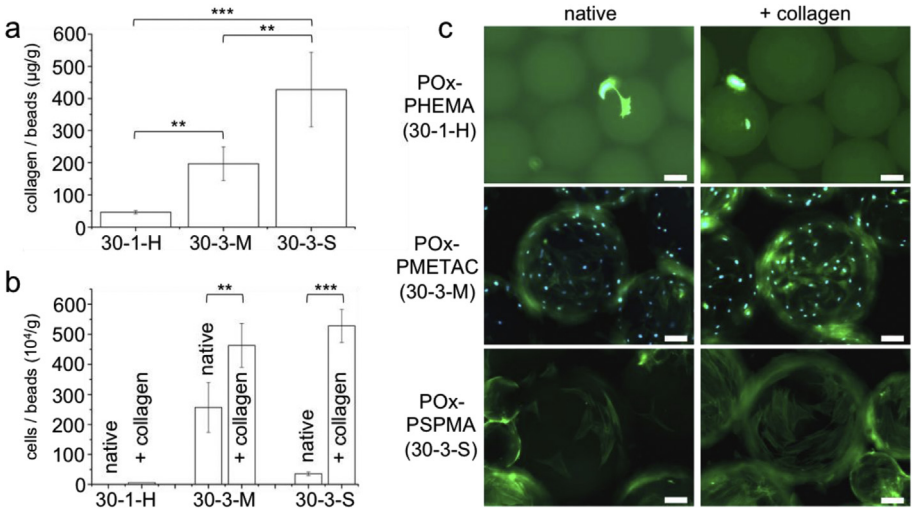

Fig. 8. Adhesion of hMSCs on native and collagen I coated $PMeOx_{30}$-PHEMA, -PMETAC and -PSPMA microbeads. a) Obtained collagen coating in µg/g microbeads as quantified by hydroxyproline assay after coating with 3 g/L collagen type I (rat tail) for 1 day and subsequent washing. b) Numbers of adhered hMSCs in 10^4 cells/g microbeads for native and collagen I coated microcarriers. c) Fluorescent micrographs of fixed and stained (Alexa 488 and DAPI) hMSCs adhered to the microcarriers after 7 days in culture. Please note that DAPI staining was not possible for PHEMA or PSPMA containing microcarriers due to strong unspecific uptake of the DAPI into the beads. Scale bar is 100 µm for all micrographs. Values are presented as mean (n = 3) ± S.D., $^{**}p < 0.05$, $^{***}p < 0.01$ using Student's *t*-test.

For the use of the POx-based microbeads in regenerative therapies, we selected a disulfide group as a central bridge of the telechelic POx linker as outlined in Fig. 5 to allow slow biodegradation of the microcarrier hydrogel under physiological conditions by glutathione (GSH) at concentrations around 2.8 µM [72]. The degradation of the hydrogel network by central chain scission of

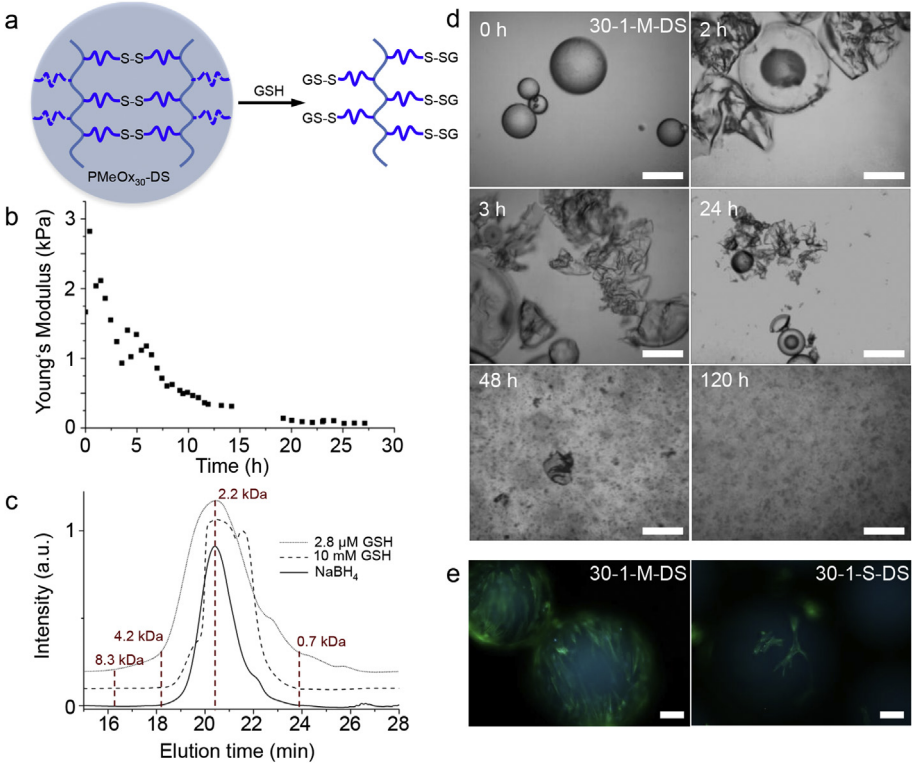

Fig. 9. Biodegradable microcarriers were prepared from $PMeOx_{30}$-DS crosslinkers with a central disulfide group and METAC monomers at a ratio of 70:30 (entry 22 in Table 2). a) In the presence of glutathione (GSH) at physiological concentrations (2.8 µM) the hydrogel microbeads disintegrate because of central chain scission of the PMeOx crosslinker to "POxylated" polymeric fragments. b) Development of the Young's modulus with the time of GSH exposure at 37 °C as probed by *in situ* colloidal probe spectroscopy of the hydrogel beads (30-1-M-DS) in the presence of 10 mM GSH to avoid additional oxidation as the CPS liquid cell could not be operated under inert conditions. c) SEC traces of degraded 30-1-M-DS microbeads after treatment of 2.8 µM GSH (solid gray line), 10 mM GSH (dashed line) and $NaBH_4$ (solid line, positive control) at 37 °C after 5 days incubation confirming almost complete degradation to molar masses lower 9 kDa. Indicated molar masses were obtained from calibration with PMeOx homopolymer standards. d) Optical micrographs of the complete disintegration of 30-1-M-DS microbeads in 2.8 µM GSH solution at 37 °C at indicated time points. Scale bars are 100 µm e) Fluorescence micrographs of fixed and stained (Alexa 488 and DAPI) hMSCs on degradable microcarriers after 7 days in culture. Scale bars are 100 µm.

the PMeOx crosslinker is schematically outlined in Fig. 9a. Most importantly, the resulting polymeric degradation products will still be side chain substituted with short PMeOx chains and possibly of relatively low molar mass. Detailed studies have showed that PMeOx conjugates exhibit the so-called *stealth effect* which significantly prolongs the blood circulation time of POx-conjugates [33] and strongly reduces their immunogenicity [16] as well as toxicity [73]. Furthermore, PMeOx itself is hemocompatible [74], non-toxic [30] and hydrophilic PMeOx is readily cleared from the body by renal excretion [32]. Hence, hydrogel disintegration by central PMeOx chain scission should result in low molar mass, biocompatible and water soluble polymer fragments that can be excreted. This may even apply for the positively charged POx-PMETAC fragments. Normally, polycationic compounds show substantial cytotoxicity but it was recently found that polycations liked to PMeOx show low to none cytotoxicity even at high concentrations as well as low serum protein binding [73].

First, the degradation of 30-1-M-DS type microbeads (entry 22 in Table 2) by GSH for 5 days was studied by optical microscopy under exclusion of oxygen at body temperature (schematic reaction Fig. 9a). The GSH concentration was set to 2.8 μM as a typical physiological concentration found for e.g. extracellular rat brain fluid [72] since in additional work we report on the use of POx-based microbeads for neuronal cell culture [75]. The series of micrographs in Fig. 9d show the complete structural disintegration of the beads. Already after 2 h, no more structurally intact particles could be found but mostly larger fragments. The particle disintegration continues steadily until after 2–3 days only very small fragments could be found. Finally, after 5 days the microbeads were transformed into a homogeneous solution without detectable microscopic fragments.

Additionally, the progression of the network degradation was investigated with respect to the changes of the Young's modulus of individual hydrogel microbeads by means of *in situ* CPS. Here, the GSH concentration had to be set to 10 mM to significantly reduce the degradation time from several days to 27 h and to minimize effects of GSH oxidation as the AFM liquid cell could not be operated under strict inert conditions and to allow for consistent elasticity measurements. Fig. 9b shows the significant reduction of the Young's modulus during the GSH mediated degradation. The initial elasticity of 2–3 kPa was dramatically reduced within the first 7 h to 0.5 kPa and within 17 h slowly dropped to around 100 Pa until no more fragments could be found for meaningful elasticity measurements. For comparison, CPS measurements on microbeads of the very same batch were performed in the absence of GSH. The negative control gave intact and unchanged microbeads after several days at 37 °C in buffer with no noticeable change of their elasticity. Thus, it can be concluded that in the absence of GSH the particles are stable.

Furthermore, we investigated the molar masses of the water soluble polymeric fragments of the microbeads after GSH mediated degradation (Fig. 9c) by size exclusion chromatography (SEC). As these metabolic compounds would eventually enter the blood circulation, their mass should be below the renal excretion threshold to avoid or minimize unspecific organ deposition. The 30-1-M-DS particles were degraded at the different GSH concentrations (physiological 2.8 μM and 10 mM as used in the CPS experiment) and, for comparison, by a strong reducing agent, sodium borohydride (0.5 M) for 5 days at 37 °C. After the GSH incubation the resulting crude solution was analyzed by SEC calibrated by PMeOx homopolymers in the range between 0.95 and 16.5 kDa (Fig. 9c). Reductive degradation of the microbeads by sodium borohydride resulted in a complete disintegration of the beads to surprisingly low molar mass polymeric fragments. The relatively defined elution peak has a maximum around t = 21.5 min which corresponds to a molar mass of only ≈2.2 kDa. The 30-1-M-DS material degraded by GSH gave broader and increasingly multimodal distributions but with elution peak maxima corresponding to the same molar mass. A second peak maximum around t = 22 min (M = 1.43 kDa) is visible for degradation products with 10 mM GSH. Overall, the water soluble polymer fragments from both experiments with GSH were found to have molar masses below 8.3 kDa and are thus way below the renal excretion limit of around 30–50 kDa [76]. Finally, we performed control experiments with the degradable positively and negatively charged microbeads (30-1-M-DS and 30-1-S-DS) to exclude an influence of the introduced disulfide bond in the POx-linker on the cell colonization and verify the stability of the microbeads under cell culture conditions. As apparent from the fluorescence micrographs in Fig. 9e, both types of beads were stable under cell culture conditions for at least 7 days and hMSCs colonization was very similar to the analog microbeads without the disulfide group.

The GSH-triggered degradation of disulfide-bridged POx-microbeads is not only an intriguing material for regenerative therapies but may also facilitate cell harvesting.

4. Conclusion

In this work we present the synthesis of hydrogel microbeads based on telechelic poly(2-oxazoline) (POx) crosslinkers and the methacrylate monomers HEMA, METAC and SPMA. While emulsion polymerization in batch gave irregular beads of undefined size, emulsion polymerization in a microfluidic (MF) device resulted in homogeneous and regular beads with narrow size distributions and also allows the fabrication of microbeads in a continuous manner with an output of approx. 3–4 g/h. Variation of the MF parameters controlled the microbead size from 50 to 500 μm. Microbead elasticity could be tuned from 2 to 20 kPa by the POx:comonomer composition, the POx chain length, net charge of the hydrogel introduced via the comonomer and the organic content in the water phase. The proliferation of human mesenchymal stem cells (hMSCs) on the microbeads were studied. While neutral, hydrophilic POx-PHEMA beads were bioinert, excessive colonization of hMSCs on charged POx-PMETAC and POx-PSPMA were found. The number of adhered cells scaled roughly linear with the METAC or SPMA to POx ratio. Additional collagen I coating further improved the stem cell colonization on the hydrogel microbeads. Finally, a first biodegradable hydrogel microcarrier system based on poly(2-oxazoline)s is described for the use in regenerative therapies which should allow *ex vivo* culturing, transplantation and GSH-trigged degradation of the beads into small polymeric fragments with molar masses way below the renal excretion threshold. The biodegradable POx-microcarriers are also of interest for continuous cell proliferation in bioreactors.

Acknowledgments

This work was supported by grant to S.P. from the Deutsche Forschungsgemeinschaft (FZ 111) and from the Cluster of Excellence “Center for Regenerative Therapies Dresden” (CRTD) Seed Grant program (to S. P. and R. J.). R.J. acknowledge additional support by the National Institutes of Health through the National Cancer Institute Alliance for Nanotechnology in Cancer (UO1 CA151806) and by funding of the Excellence Initiative by the German Federal and State Governments” (Institutional Strategy, measure “support the best”).

References

[1] E. Tumarkin, E. Kumacheva, Microfluidic generation of microgels from

synthetic and natural polymers, Chem. Soc. Rev. 38 (8) (2009) 2161–2168.
[2] M.J. Murray, M.J. Snowden, The preparation, characterisation and applications of colloidal microgels, Adv. Colloid Interf. Sci. 54 (1995) 73–91.
[3] J.B. Thorne, G.J. Vine, M.J. Snowden, Microgel applications and commercial considerations, Colloid Polym. Sci. 289 (5–6) (2011) 625–646.
[4] A.V. Kabanov, S.V. Vinogradov, Nanogels as pharmaceutical carriers: finite networks of infinite capabilities, Angew. Chem. Int. Ed. 48 (30) (2009) 5418–5429.
[5] F. Pampaloni, E.G. Reynaud, E.H.K. Stelzer, The third dimension bridges the gap between cell culture and live tissue, Nat. Rev. Mol. Cell Biol. 8 (10) (2007) 839–845.
[6] S. Pautot, C. Wyart, E.Y. Isacoff, Colloid-guided assembly of oriented 3d neuronal networks, Nat. Methods 5 (8) (2008) 735–740.
[7] D. Jgamadze, J. Bergen, D. Stone, J.-H. Jang, D.V. Schaffer, E.Y. Isacoff, S. Pautot, Colloids as mobile substrates for the implantation and integration of differentiated neurons into the mammalian brain, PloS One 7 (1) (2012) e30293.
[8] C.J. Hewitt, K. Lee, A.W. Nienow, R.J. Thomas, M. Smith, C.R. Thomas, Expansion of human mesenchymal stem cells on microcarriers, Biotechnol. Lett. 33 (11) (2011) 2325–2335.
[9] Y. Yuan, M.S. Kallos, C. Hunter, A. Sen, Improved expansion of human bone marrow-derived mesenchymal stem cells in microcarrier-based suspension culture, J. Tissue Eng. Regen. Med. 8 (3) (2012) 210–225.
[10] K.W. Chun, H.S. Yoo, J.J. Yoon, T.G. Park, Biodegradable PLGA microcarriers for injectable delivery of chondrocytes: effect of surface modification on cell attachment and function, Biotechnol. Prog. 20 (6) (2004) 1797–1801.
[11] A.K.A.S. Brun-Graeppi, C. Richard, M. Bessodes, D. Scherman, O.-W. Merten, Cell microcarriers and microcapsules of stimuli-responsive polymers, J. Control. Release 149 (3) (2011) 209–224.
[12] S. Allazetta, T.C. Hausherr, M.P. Lutolf, Microfluidic synthesis of cell-type-specific artificial extracellular matrix hydrogels, Biomacromolecules 14 (4) (2013) 1122–1131.
[13] D. Jgamadze, L. Liu, S. Vogler, L.-Y. Chu, S. Pautot, Thermoswitching microgel carriers improve neuronal cell growth and cell release for cell transplantation, Tissue Eng. Part C Methods 21 (1) (2014) 65–76.
[14] K. Aoi, M. Okada, Polymerization of oxazolines, Prog. Polym. Sci. 21 (1996) 151–208.
[15] F. Rehfeldt, M. Tanaka, L. Pagnoni, R. Jordan, Static and dynamic swelling of grafted poly(2-alkyl-2-oxazoline)s, Langmuir 18 (12) (2002) 4908–4914.
[16] T.X. Viegas, M.D. Bentley, J.M. Harris, Z. Fang, K. Yoon, B. Dizman, et al., Polyoxazoline: chemistry, properties, and applications in drug delivery, Bioconjug. Chem. 22 (5) (2011) 976–986.
[17] T.B. Bonne, K. Lüdtke, R. Jordan, P. Stepanek, C.M. Papadakis, Aggregation behavior of amphiphilic poly(2-alkyl-2-oxazoline) diblock copolymers in aqueous solution studied by fluorescence correlation spectroscopy, Colloid Polym. Sci. 282 (8) (2004) 833–843.
[18] M.B. Foreman, J.P. Coffman, M.J. Murcia, S. Cesana, R. Jordan, G.S. Smith, C.A. Naumann, Gelation of amphiphilic lipopolymers at the air-water interface: 2D analogue to 3d gelation of colloidal systems with grafted polymer chains? Langmuir 19 (2) (2003) 326–332.
[19] S. Cesana, J. Auernheimer, R. Jordan, H. Kessler, O. Nuyken, First poly(2-oxazoline)s with pendant amino groups, Macromol. Chem. Phys. 207 (2) (2006) 183–192.
[20] C. Taubmann, R. Luxenhofer, S. Cesana, R. Jordan, First aldehyde-functionalized poly(2-oxazoline)s for chemoselective ligation, Macromol. Biosci. 5 (7) (2005) 603–612.
[21] A. Levy, M. Litt, Polymerization of cyclic iminoethers. V. 1,3-oxazolines with hydroxy-, acetoxy-, and carboxymethyl-alkyl groups in the 2 position and their polymers, J. Polym. Sci. Part A 1 Polym. Chem. 6 (1968) 1883–1894.
[22] R. Luxenhofer, R. Jordan, Click chemistry with poly(2-oxazoline)s, Macromolecules 39 (10) (2006) 3509–3516.
[23] K. Kempe, M. Lobert, R. Hoogenboom, U.S. Schubert, Screening the synthesis of 2-substituted-2-oxazolines, J. Comb. Chem. 11 (2) (2009) 274–280.
[24] R. Luxenhofer, M. Bezen, R. Jordan, Kinetic investigations on the polymerization of 2-oxazolines using pluritriflate initators, Macromol. Rapid Commun. 29 (18) (2008) 1509–1513.
[25] M.W.M. Fijten, C. Haensch, B.M. van Lankvelt, R. Hoogenboom, U.S. Schubert, Clickable poly(2-oxazoline)s as versatile building blocks, Macromol. Chem. Phys. 209 (18) (2008) 1887–1895.
[26] N. Zhang, S. Huber, A. Schulz, R. Luxenhofer, R. Jordan, Cylindrical molecular brushes of poly(2-oxazoline)s from 2-isopropenyl-2-oxazoline, Macromolecules 42 (6) (2009) 2215–2221.
[27] N. Zhang, R. Luxenhofer, R. Jordan, Thermoresponsive poly(2-oxazoline) molecular brushes by living ionic polymerization: kinetic investigations of pendant chain grafting and cloud point modulation by backbone and side chain length variation, Macromol. Chem. Phys. 213 (9) (2012) 973–981.
[28] N. Zhang, R. Luxenhofer, R. Jordan, Thermoresponsive poly(2-oxazoline) molecular brushes by living ionic polymerization: modulation of the cloud point by random and block copolymer pendant chains, Macromol. Chem. Phys. 213 (18) (2012) 1963–1969.
[29] J. Bühler, S. Gietzen, A. Reuter, C. Kappel, K. Fischer, S. Decker, et al., Selective uptake of cylindrical poly(2-oxazoline) brush-antidec205 antibody-ova antigen conjugates into dec-positive dendritic cells and subsequent t-cell activation, Chemistry 20 (39) (2014) 12405–12410.
[30] R. Luxenhofer, G. Sahay, A. Schulz, D. Alakhova, T.K. Bronich, R. Jordan, A.V. Kabanov, Structure-property relationship in cytotoxicity and cell uptake of poly(2-oxazoline) amphiphiles, J. Control. Release 153 (1) (2011) 73–82.
[31] R. Luxenhofer, A. Schulz, C. Roques, S. Li, T.K. Bronich, E.V. Batrakova, et al., Doubly-amphiphilic poly(2-oxazoline)s as high-capacity delivery systems for hydrophobic drugs, Biomaterials 31 (18) (2010) 4972–4979.
[32] F.C. Gaertner, R. Luxenhofer, B. Blechert, R. Jordan, M. Essler, Synthesis, biodistribution and excretion of radiolabeled poly(2-alkyl-2-oxazoline)s, J. Control. Release 119 (3) (2007) 291–300.
[33] M.C. Woodle, C.M. Engbers, S. Zalipsky, New amphipatic polymer-lipid conjugates forming long-circulating reticuloendothelial system-evading liposomes, Bioconj. Chem. 5 (1994) 493–496.
[34] R. Hoogenboom, Poly(2-oxazoline)s: a polymer class with numerous potential applications, Angew. Chem. Int. Ed. 48 (43) (2009) 7978–7994.
[35] N. Adams, U.S. Schubert, Poly(2-oxazolines) in biological and biomedical application contexts, Adv. Drug Deliv. Rev. 59 (2007) 1504–1520.
[36] R. Luxenhofer, Y. Han, A. Schulz, J. Tong, Z. He, A.V. Kabanov, R. Jordan, Poly(2-oxazoline)s as polymer therapeutics, Macromol. Rapid Commun. 33 (19) (2012) 1613–1631.
[37] A.M. Kelly, F. Wiesbrock, Strategies for the synthesis of poly(2-oxazoline)-based hydrogels, Macromol. Rapid Commun. 33 (19) (2012) 1632–1647.
[38] U.S. Schubert, M. Hartlieb, K. Kempe, Covalently cross-linked poly (2-oxazoline) materials for biomedical applications-from hydrogels to self-assembled and templated structures, J. Mater. Chem. B 3 (4) (2014) 526–538.
[39] D. Taton, S. Lecommandoux, K.C. Tam, M.-C. De Pauw-Gillet, C. Legros, PH and redox responsive hydrogels and nanogels made from poly (2-ethyl-2-oxazoline), Polym. Chem. 4 (17) (2013) 4801–4808.
[40] T.R. Dargaville, R. Forster, B.L. Farrugia, K. Kempe, L. Voorhaar, U.S. Schubert, R. Hoogenboom, Poly(2-oxazoline) hydrogel monoliths via thiol-ene coupling, Macromol. Rapid Commun. 33 (19) (2012) 1695–1700.
[41] G. David, B.C. Simionescu, A.-C. Albertsson, Rapid deswelling response of poly(n-isopropylacrylamide)/poly(2-alkyl-2-oxazoline)/poly(2-hydroxyethyl methacrylate) hydrogels, Biomacromolecules 9 (6) (2008) 1678–1683.
[42] S. Zschoche, J. Rueda, V. Boyko, F. Krahl, K.F. Arndt, B. Voit, Thermo-responsive nanogels based on poly[nipaam-graft-(2-alkyl-2-oxazoline)]s crosslinked in the micellar state, Macromol. Chem. Phys. 211 (9) (2010) 1035–1042.
[43] C. Legros, A.-L. Wirotius, M.-C. De Pauw-Gillet, K.C. Tam, D. Taton, S. Lecommandoux, Poly(2-oxazoline)-based nanogels as biocompatible pseudopolypeptide nanoparticles, Biomacromolecules 16 (1) (2014) 183–191.
[44] V.V. Jerca, F.A. Nicolescu, R. Trusca, E. Vasile, A. Baran, D.F. Anghel, et al., Oxazoline-functional polymer particles graft with azo-dye, React. Funct. Polym. 71 (4) (2011) 373–379.
[45] D.C. Duffy, J.C. McDonald, O.J. Schueller, G.M. Whitesides, Rapid prototyping of microfluidic systems in poly(dimethylsiloxane), Anal. Chem. 70 (23) (1998) 4974–4984.
[46] R.K. Shah, J.W. Kim, J.J. Agresti, D.A. Weitz, L.Y. Chu, Fabrication of monodisperse thermosensitive microgels and gel capsules in microfluidic devices, Soft Matter 4 (12) (2008) 2303–2309.
[47] B.G. De Geest, J.P. Urbanski, T. Thorsen, J. Demeester, S.C. De Smedt, Synthesis of monodisperse biodegradable microgels in microfluidic devices, Langmuir 21 (23) (2005) 10275–10279.
[48] J.P. Best, J. Cui, M. Müllner, F. Caruso, Tuning the mechanical properties of nanoporous hydrogel particles via polymer cross-linking, Langmuir 29 (31) (2013) 9824–9831.
[49] D.E. Discher, P. Janmey, Y.-L. Wang, Tissue cells feel and respond to the stiffness of their substrate, Science 310 (5751) (2005) 1139–1143.
[50] A.J. Engler, S. Sen, H.L. Sweeney, D.E. Discher, Matrix elasticity directs stem cell lineage specification, Cell 126 (4) (2006) 677–689.
[51] A.J. Engler, F. Rehfeldt, S. Sen, D.E. Discher, Microtissue elasticity: measurements by atomic force microscopy and its influence on cell differentiation, Cell Mech. 83 (2007) 521–545.
[52] B. Trappmann, J.E. Gautrot, J.T. Connelly, D.G.T. Strange, Y. Li, M.L. Oyen, et al., Extracellular-matrix tethering regulates stem-cell fate, Nat. Mater. 11 (7) (2012) 642–649.
[53] S. Schmidt, M. Zeiser, T. Hellweg, C. Duschl, A. Fery, H. Möhwald, Adhesion and mechanical properties of pnipam microgel films and their potential use as switchable cell culture substrates, Adv. Funct. Mater. 20 (19) (2010) 3235–3243.
[54] G. Kesava Reddy, C.S. Enwemeka, A simplified method for the analysis of hydroxyproline in biological tissues, Clin. Biochem. 29 (3) (1996) 225–229.
[55] D. Christova, R. Velichkova, W. Loos, E.J. Goethals, F. du Prez, New thermo-responsive polymer materials based on poly (2-ethyl-2-oxazoline) segments, Polymer 44 (8) (2003) 2255–2261.
[56] D. Christova, R. Velichkova, E.J. Goethals, F.E. Du Prez, Amphiphilic segmented polymer networks based on poly (2-alkyl-2-oxazoline) and poly (methyl methacrylate), Polymer 43 (17) (2002) 4585–4590.
[57] S. Kobayashi, H. Uyama, Y. Narita, J. Ishiyama, Novel multifunctional initiators for polymerization of 2-oxazolines, Macromolecules 25 (12) (1992) 3232–3236.
[58] S.J. Kim, K.J. Lee, I.Y. Kim, D.I. Shin, S.I. Kim, Temperature and ph-response swelling behavior of poly (2-ethyl-2-oxazoline)/chitosan interpenetrating polymer network hydrogels, J. Appl. Polym. Sci. 99 (3) (2006) 1100–1103.
[59] B. Kostova, S. Ivanova, K. Balashev, D. Rachev, D. Christova, Evaluation of poly(2-ethyl-2-oxazoline) containing copolymer networks of varied composition as sustained metoprolol tartrate delivery systems, AAPS PharmSciTech 15 (4) (2014) 939–946.
[60] J.K. Oh, R. Drumright, D.J. Siegwart, K. Matyjaszewski, The development of

microgels/nanogels for drug delivery applications, Prog. Polym. Sci. 33 (4) (2008) 448–477.
[61] D. Dhananjay, D.C. Pregibon, J. Collins, T.A. Hatton, P. Doyle, Continuous-flow lithography for high-throughput microparticle synthesis, Nat. Mater. 5 (2006) 365–369.
[62] M. Kappl, H.J. Butt, The colloidal probe technique and its application to adhesion force measurements, Part. Syst. Charact. 19 (3) (2002) 129–143.
[63] H.-J. Butt, B. Cappella, M. Kappl, Force measurements with the atomic force microscope: Technique, interpretation and applications, Surf. Sci. Rep. 59 (1) (2005) 1–152.
[64] A.J. Engler, M.A. Griffin, S. Sen, C.G. Bönnemann, H.L. Sweeney, D.E. Discher, Myotubes differentiate optimally on substrates with tissue-like stiffness: pathological implications for soft or stiff microenvironments, J. Cell Biol. 166 (6) (2004) 877–887.
[65] B.L. Farrugia, K. Kempe, U.S. Schubert, R. Hoogenboom, T.R. Dargaville, Poly(2-oxazoline) hydrogels for controlled fibroblast attachment, Biomacromolecules 14 (8) (2013) 2724–2732.
[66] A.S. Rowlands, P.A. George, J.J. Cooper-White, Directing osteogenic and myogenic differentiation of mscs: interplay of stiffness and adhesive ligand presentation, Am. J. Physiol. Cell Physiol. 295 (4) (2008) C1037–C1044.
[67] K. Johnson, S. Zhu, M.S. Tremblay, J.N. Payette, J. Wang, L.C. Bouchez, et al., A stem cell-based approach to cartilage repair, Science 336 (6082) (2012) 717–721.
[68] T. Liao, M.D. Moussallem, J. Kim, J.B. Schlenoff, T. Ma, N-isopropylacrylamide-based thermoresponsive polyelectrolyte multilayer films for human mesenchymal stem cell expansion, Biotechnol. Prog. 26 (6) (2010) 1705–1713.
[69] A.P. Ngankam, G. Mao, P.R. Van Tassel, Fibronectin adsorption onto polyelectrolyte multilayer films, Langmuir 20 (8) (2004) 3362–3370.
[70] R. Konradi, B. Pidhatika, A. Mühlebach, M. Textor, Poly-2-methyl-2-oxazoline: a peptide-like polymer for protein-repellent surfaces, Langmuir 24 (3) (2008) 613–616.
[71] N. Zhang, T. Pompe, I. Amin, R. Luxenhofer, C. Werner, R. Jordan, Tailored poly(2-oxazoline) polymer brushes to control protein adsorption and cell adhesion, Macromol. Biosci. 12 (2012) 926–936.
[72] C.-S. Yang, S.-T. Chou, N.-N. Lin, L. Liu, P.-J. Tsai, J.-S. Kuo, J.-S. Lai, Determination of extracellular glutathione in rat brain by microdialysis and high-performance liquid chromatography with fluorescence detection, J. Chromatogr. B 661 (2) (1994) 231–235.
[73] Z. He, L. Miao, R. Jordan, D. S-Manickam, R. Luxenhofer, A.V. Kabanov, A low protein binding cationic poly(2-oxazoline) as non-viral vector, Macromol. Biosci. 15 (7) (2015) 1004–1020.
[74] M. Bauer, S. Schroeder, L. Tauhardt, K. Kempe, U.S. Schubert, D. Fischer, In vitro hemocompatibility and cytotoxicity study of poly (2-methyl-2-oxazoline) for biomedical applications, J. Polym. Sci. Part A Polym. Chem. 51 (8) (2013) 1816–1821.
[75] M. Platen, E. Mathieu, S. Lück, R. Schubel, R. Jordan, S. Pautot, Poly(2-oxazoline) based microbeads for neuronal cell culture, Biomacromolecules 16 (5) (2015) 1516–1524.
[76] M.E. Fox, F.C. Szoka, J.M. Fréchet, Soluble polymer carriers for the treatment of cancer: The importance of molecular architecture, Acc. Chem. Res. 42 (8) (2009) 1141–1151.